

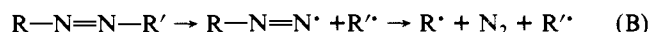
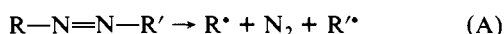
Time-Resolved Observation of Sequential Bond Cleavage in a Gas-Phase Azoalkane

J. Stephen Adams, Katherine A. Burton, B. Kim Andrews, R. Bruce Weisman,* and Paul S. Engel*

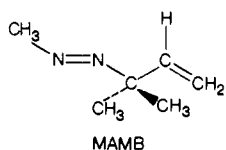
Contribution from the Department of Chemistry and Rice Quantum Institute, Rice University, Houston, Texas 77251. Received July 25, 1986

Abstract: The gas-phase photodissociation of an unsymmetrical azoalkane, 3-(methylazo)-3-methyl-1-butene, was studied with time-resolved coherent anti-Stokes Raman spectroscopy (CARS) to probe for product formation. Appearance kinetics were measured for all three primary photoproducts. The results indicate a two-step dissociation mechanism in which the 1,1-dimethylallyl fragment is formed within 2 ns of excitation, whereas the methyl radical and N₂ are formed through decay of a reaction intermediate having a lifetime of 12 ± 2 ns. These findings mark the first direct demonstration of a stepwise homolysis mechanism for an azoalkane.

The characteristic tendency of azoalkanes to dissociate under the influence of light or heat has for decades made this class of compounds a useful source of alkyl radicals as well as an attractive subject for mechanistic study.¹ Despite the fact that a wide variety of physical-organic techniques have been brought to bear on the question of the homolysis mechanism, it has remained unresolved as to whether azoalkanes dissociate by simultaneous (A) or stepwise (B) bond cleavage.



In the period since the 1980 review of research in this area,¹ Engel and co-workers have addressed the limitations of using thermolysis rates as a mechanistic probe² and have also reported the formation of "turnaround" photoproducts from unsymmetrical allylic azoalkanes such as 3-(methylazo)-3-methyl-1-butene (MAMB).³ This result strongly supports the stepwise mechanism



involving diazenyl radical intermediates, R-N=N[•], for solution-phase dissociations in which R is an unstabilized radical. Other recent evidence favoring stepwise dissociation includes analysis of pressure-dependent solution-phase thermolysis rates,⁴ molecular orbital calculations of potential energy surfaces,⁵ secondary deuterium isotope effects in 4-alkylidene-1-pyrazolines,⁶ and a gas-phase study of 2,3-diazabicyclo[2.1.1]hex-2-ene.⁷

In our 1985 study of azomethane vapor (CH₃-N=N-CH₃),⁸ we used transient CARS (coherent anti-Stokes Raman spectroscopy) as a time-resolved vibrational probe of the photoproducts formed after ultraviolet excitation. Although significant information was gained about the internal energy contents of the products, we did not find kinetic evidence for stepwise dissociation on a time scale resolvable with our apparatus.

We report here the results of further direct gas-phase kinetic measurements using ultraviolet sample excitation followed by

vibrational spectroscopic detection of products. The unsymmetrical azoalkane MAMB was studied with this method and found to show resolvable stepwise dissociation. We believe that this finding, which is the first time-regime determination of mechanism for an azo dissociation, clearly establishes the stepwise pathway for unsymmetrical azoalkanes and also demonstrates consistency between the gas- and solution-phase behaviors.

Experimental Section

Our time-resolved CARS measurements were made with an apparatus that uses one Q-switched Nd:YAG laser system to generate an ultraviolet excitation pulse and a second Nd:YAG-pumped dye laser system for pulsed probing of the excited sample. The home-made lasers were very similar to the description reported earlier;⁹ the major difference was that our probing YAG laser was operated as a stable TEM₀₀ oscillator with a single-pass amplifier. The azoalkane samples were excited at 355 nm with YAG third harmonic pulses having typical energies of 10 mJ. Following a selectable nanosecond-scale time delay, the probing laser system generated two synchronized visible pulses whose frequency difference was set to the vibrational Raman frequency of interest. One of these beams, ω₁, was the 532-nm YAG second harmonic, while the other, ω₂, was the tunable output of a dye laser operating with Rhodamine 640 or DCM. As shown in Figure 1, these two probing beams were collinearly combined and directed through the sample volume excited by the ultraviolet beam. Light generated at the frequency 2ω₁-ω₂ by the sample's CARS susceptibility emerged collinearly with the intense probe beams. This weak signal beam was passed through dielectric short pass filters to attenuate ω₁ and ω₂ components, focused through a 35 μm diameter pinhole to block ultraviolet-induced luminescence generated in the cell window, and directed through a small tunable grating filter for further spectral selection.

The CARS beam was detected by a Hamamatsu R1477 photomultiplier, whose anode photocurrent was integrated with an Evans Associates Model 4130 gated integrator and digitized by the 12 bit A/D converter board of our laboratory computer. This computer, based on a DEC 11/73-series processor, monitored the CARS signal and laser energies for each shot, controlled the delay between excitation and probe lasers, and set the frequency of the probe laser. In order to distinguish photoproduct CARS signals from ground-state features, the probe delay was switched between positive and negative values on alternate laser shots and the square root of the negative-delay signal was subtracted from the square root of the positive-delay signal. Since CARS intensities vary as the square of the sample concentration,¹⁰ this procedure gave a value proportional to the concentration of the transient species at the selected positive delay time (assuming small nonresonant backgrounds). Because the CARS process is highly nonlinear, fluctuations in the energies and spatial character of the probe beams can lead to substantial noise in the CARS signal. We reduced this noise through shot-by-shot normalization either to the CARS signal generated in a reference cell containing 11 atm of argon (a nonresonant standard) or to the product of the ω₂ energy and

(1) Engel, P. S. *Chem. Rev.* **1980**, *80*, 99.

(2) Engel, P. S.; Nalepa, C. J.; Horsey, D. W.; Keys, D. E.; Grow, R. T. *J. Am. Chem. Soc.* **1983**, *105*, 7102.

(3) Engel, P. S.; Gerth, D. B. *J. Am. Chem. Soc.* **1983**, *105*, 6849.

(4) Neuman, R. C.; Binegar, G. A. *J. Am. Chem. Soc.* **1983**, *105*, 134.

(5) (a) Dannenberg, J. J. *J. Org. Chem.* **1985**, *50*, 4963. (b) Dannenberg, J. J.; Rocklin, D. *J. Org. Chem.* **1982**, *47*, 4529.

(6) (a) Crawford, R. J.; Chang, M. H. *Tetrahedron* **1982**, *38*, 837. (b) Lefevre, G. N.; Crawford, R. J. *J. Am. Chem. Soc.* **1986**, *108*, 1019.

(7) Chang, M. H.; Jain, R.; Dougherty, D. A. *J. Am. Chem. Soc.* **1986**, *106*, 4211.

(8) Holt, P. L.; McCurdy, K. E.; Adams, J. S.; Burton, K. A.; Weisman, R. B.; Engel, P. S. *J. Am. Chem. Soc.* **1985**, *107*, 2180.

(9) Weisman, R. B.; Selco, J. I.; Holt, P. L.; Cahill, P. A. *Rev. Sci. Instrum.* **1983**, *54*, 284.

(10) See, for example: Nibler, J. W.; Knight, G. V. In *Raman Spectroscopy of Gas and Liquids*; Weber, A., Ed.; Springer-Verlag: Berlin, 1979; p 253. Tolles, W. M.; Nibler, J. W.; McDonald, J. R.; Harvey, A. B. *Appl. Spectrosc.* **1977**, *31*, 253.

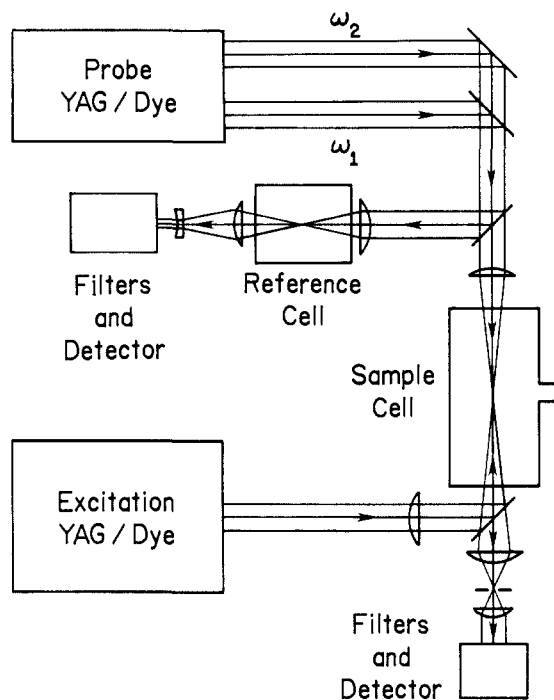


Figure 1. Optical schematic diagram of the transient CARS apparatus. Many individual optical elements have been omitted for clarity, and none of the electronics or computer components are shown.

the squared ω_1 energy for that shot. To account for fluctuations in the number of excitation photons per pulse, we then divided by the ultraviolet beam energy during each cycle of data acquisition. Our kinetic data were obtained by recording the processed CARS signal as a function of probe delay for a fixed Raman probe frequency; transient spectra were measured by scanning the probe frequency with the positive probe delay held constant. Our instrumental spectral resolution was 1 cm^{-1} , and the time profile was approximately 8 ns in width.

The sample cell was 60 cm long and 2 cm in diameter. It was equipped with dichroic entrance and exit windows (to exclude nonresonant and atmospheric CARS backgrounds) and capacitance pressure gauges. With the cell filled with the desired static pressure of azoalkane sample and buffer gas, the sample concentration within the probed volume was replenished by diffusional motion during the 100-ms interval between laser shots. We performed data scans on each sample fill until a significant fraction of the sample in the cell had been photolyzed. The cell was then evacuated and refilled. All measurements were made at $23 \pm 2 \text{ }^\circ\text{C}$.

MAMB was prepared by sodium hypochlorite oxidation of the sulfamide derived from 3-amino-3-methyl-1-butene and methylsulfamoyl chloride.¹¹ The product was purified by drying over Na_2SO_4 , followed by bulb-to-bulb distillation ($25 \text{ }^\circ\text{C}$ (60 mmHg)) to a $-196 \text{ }^\circ\text{C}$ trap; yield 47%. NMR and UV spectra confirmed that our product was identical with the material prepared earlier.^{3,11} 3-Azobis(3-methyl-1-butene) (AMB) was synthesized according to the literature, and its NMR spectrum matched those reported previously.^{3,11}

Results and Discussion

We first investigated the ultraviolet-induced transient CARS spectrum of MAMB in the C-H stretching region under rotationally relaxed conditions. Using a sample of 2.0 Torr of MAMB and 145 Torr of helium buffer gas, we observed the induced CARS spectrum shown in Figure 2 at a probe delay of 30 ns. Several features of this spectrum are significant. The strongest peak, centered near 3002 cm^{-1} , is clearly the ν_1 band of methyl radicals.¹² The sharp dip at 2997 cm^{-1} corresponds to a ground-state MAMB transition. This feature is easily understood, since partial depletion of the ground-state population by the excitation pulse will give a negative-going contribution to the induced CARS spectrum for all ground-state bands of the azo sample. At frequencies below

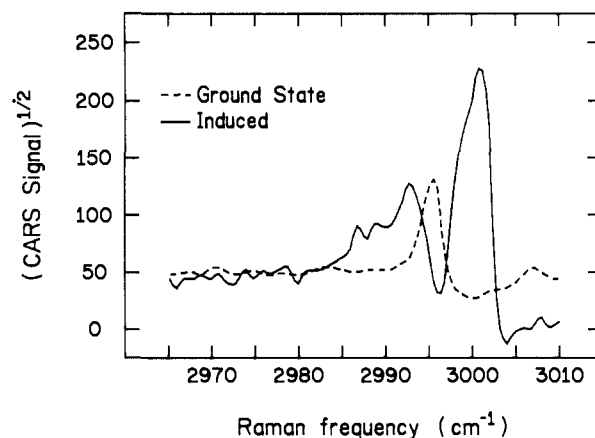


Figure 2. Ground-state (---) and transient (—) CARS spectra of a sample of 2.0 Torr of MAMB and 145 Torr of helium. The probe beam was delayed 30 ns from excitation for the transient spectrum.

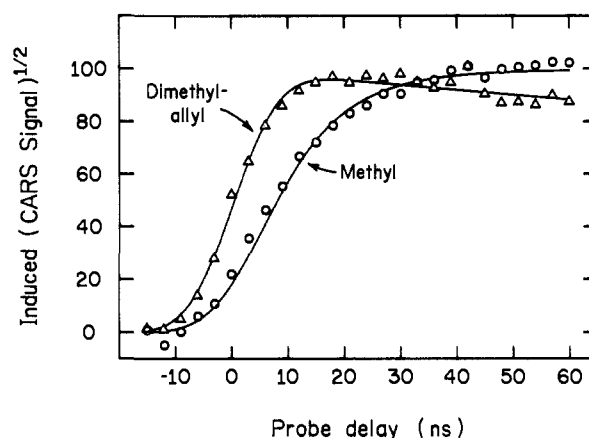
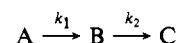


Figure 3. Kinetics of the transient CARS signals observed at 2993 cm^{-1} (Δ) and 3002 cm^{-1} (\circ) in a sample containing 2 Torr of MAMB and 100 Torr of helium. The solid curves are best fits computed with the kinetic model described in the text.

2980 cm^{-1} we find a positive, spectrally flat component that is also evident in the 3050 to 3200 cm^{-1} range, where ground-state features are not obtrusive. We assign this plateau to a nonresonant CARS background from a transient species. The final significant feature of the induced spectrum is the band centered near 2993 cm^{-1} , which is evidently a vibrational transition of a transient. From its closeness to the methyl peak, one might suspect a vibrational hot band of the methyl radical. However, we exclude this possibility because the band is not quenched in the presence of 80 Torr of SF_6 at a delay of 125 ns. Judging from our studies of hot bands in methyl radicals formed from azomethane,¹³ vibrational relaxation should be complete under these conditions. The band near 2993 cm^{-1} must therefore be a transition of a relaxed species other than the methyl radical.

The next stage of investigation involved kinetic measurements of the induced CARS signals at 2993 and 3002 cm^{-1} . We recorded the early kinetics at these two frequencies in samples containing approximately 2 Torr of MAMB mixed with various pressures of helium, added for rotational thermalization of the photofragments. At a helium pressure of 100 Torr, the results shown in Figure 3 were obtained. The solid curves drawn through the data symbols are computed best fits based on the two-step kinetic model



Here k_1 represents the rate of formation of the observed transient species and k_2 accounts for its irreversible early decay. It is assumed that only species B has a significant Raman cross section

(11) Engel, P. S.; Bishop, D. J.; Page, M. A. *J. Am. Chem. Soc.* **1978**, *100*, 7009.

(12) Holt, P. L.; McCurdy, K. E.; Weisman, R. B.; Adams, J. S.; Engel, P. S. *J. Chem. Phys.* **1984**, *81*, 3349.

(13) Adams, J. S.; Burton, K. A.; Weisman, R. B.; Engel, P. S., Rice University, unpublished results.

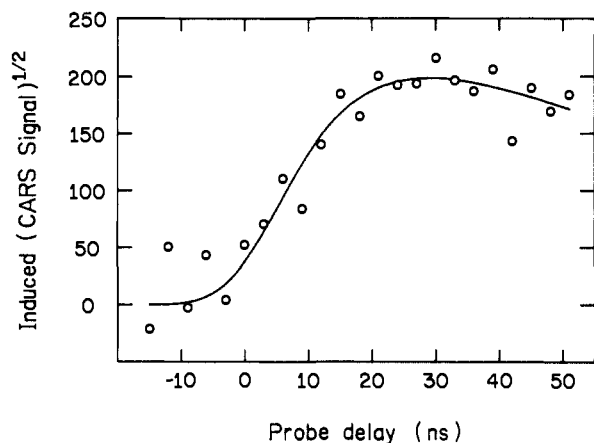
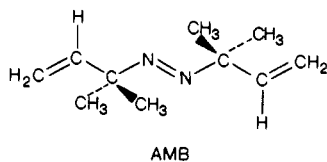


Figure 4. Kinetics of the transient CARS signal from the $v = 0-1$ Q branch of N_2 in a sample containing 2 Torr of MAMB and 250 Torr of helium. As discussed in the text, these data represent the difference of kinetic runs measured at two frequencies. The solid curve is a computed best fit.

at the probing frequency. The fit of the data at 2993 cm^{-1} gives a k_1^{-1} value of less than 1 ns, corresponding to a formation time below the resolution limit of our apparatus. By contrast, the rise kinetics at the methyl ν_1 frequency indicate a formation time, k_1^{-1} , of 12 ± 2 ns for helium buffer pressures ranging from 100 to 400 Torr. The constancy of this value over a wide range of helium pressures implies that the appearance time measured for the methyl fragment gives its true rate of formation rather than its rate of rotational thermalization to a distribution peaking at the probed frequency.

Formation kinetics of the N_2 photofragment were probed at nitrogen's well-known fundamental vibration-rotation band, whose Q branch is observed near 2330 cm^{-1} . These kinetic data were of poorer quality than those from the C-H stretching region for two reasons. First, the Raman cross section of the N_2 transition is smaller, leading to a transient spectrum that showed substantial distortion arising from interference with ground state and transient nonresonant backgrounds. To deal with this complication, we extracted the time-dependent nitrogen concentration as the difference of transient CARS signals at 2328.5 and 2332 cm^{-1} , the peak and valley frequencies of the distorted resonance band shape. A second problem was the accumulation in our static sample cell of nitrogen formed from previous laser shots. Although this background contribution was automatically subtracted during data acquisition, it contributed noise and also gave a false apparent decay of the N_2 signal that arose from the rapid density decrease in the probed volume induced by photofragment recoil. Figure 4 shows the N_2 appearance kinetics in the presence of 250 Torr of helium added for rotational thermalization. The best fit computed with the kinetic model described earlier gave a characteristic formation time, k_1^{-1} , of 13 ± 4 ns. Although this value is not as reliable as those obtained from data in the C-H stretching region, the close agreement with the methyl radical appearance time is noteworthy.

To assist in assigning the resonant 2993-cm^{-1} transient band, we examined the induced CARS spectrum of another azoalkane that is known to give only N_2 and 1,1-dimethylallyl radicals as primary photoproducts. When 3-azobis(3-methyl-1-butene) (AMB) was photolyzed at 355 nm, we observed a transient CARS



spectrum composed of a broad, apparently nonresonant positive background plus a resonant feature in the range of $2985-2995\text{ cm}^{-1}$. The presence of strong ground-state transitions of AMB in this region unfortunately made it difficult to compare the shape

of the resonant feature with that seen from photolysis of MAMB. The decay kinetics of the resonant features found near 2990 cm^{-1} from MAMB and AMB were measured and found to be very similar to each other but quite distinct from the decay of the methyl transient. On the basis of spectroscopic and kinetic comparison, it therefore appears plausible that these transient signals from the two azoalkanes arise from the same species, which would have to be the dimethylallyl radical.

Before this assignment can be considered firm, one must exclude other possible sources for the 2993-cm^{-1} transient band from MAMB. The optically excited S_1 state, of n,π^* character, can be ruled out because the fluorescence lifetime of acyclic azoalkanes is far shorter than the ca. 200 ns decay time seen for this band.¹⁴ It is believed that in this compound and in other azoalkanes, the S_1 state rapidly internally converts to high vibrational levels of S_0 .^{14,15} However, these S_0^* species cannot be the source of our transient because it is observed not to be quenched by collisions with SF_6 , an efficient vibrational relaxer. We may also rule out a triplet state of MAMB that is a direct precursor to the photofragments, since the rates of nitrogen and methyl radical formation far exceed the decay rate of the transient. A nondissociative triplet state formed from S_1 in parallel with S_0^* also seems highly unlikely in view of the short lifetimes and low formation yields characteristically found for azoalkane triplet states.¹ Finally, at the high laser intensities used for excitation, it might be possible for the S_1 state of MAMB to absorb further excitation photons and undergo a high-energy dissociation to form unexpected products. We have found, however, that in the presence of ca. 50 Torr of SF_6 , the characteristic appearance time of the 2993-cm^{-1} band is increased to approximately 30 ns. This observation may be qualitatively understood as a reduced unimolecular reaction rate accompanying vibrational cooling.¹⁶ Since the observed transient species is formed here on a time scale that is long compared to the duration of the excitation laser pulse, it cannot be a prompt product of multiphoton excitation. We conclude that none of these other possible sources can account for the 2993-cm^{-1} transient band.

Infrared absorption spectra of matrix-isolated allyl radicals provide a guide for the assignment of our observed transient band to a particular vibrational transition of the dimethylallyl radical. It has been reported that allyl radicals in an argon matrix show infrared bands at 3016 , 3048 , and 3105 cm^{-1} ,^{17,18} all of which would be expected to have some Raman activity, as well. The two additional methyl groups of the dimethylallyl radical should give vibrational transitions that fall at lower frequencies and that are nearly unshifted from the precursor's transitions. We tentatively assign our 2993-cm^{-1} transient to the symmetric CH_2 stretching vibration of the dimethylallyl radical, corresponding to the 3016-cm^{-1} band of matrix-isolated allyl. The other dimethylallyl transitions may have escaped detection either because their bands fall under ground-state features or because they have smaller Raman cross sections.

The foregoing analysis indicates that we have in fact measured the appearance rates of all three primary photoproducts of MAMB vapor. In the presence of moderate pressures of helium, we find the dimethylallyl radical to be formed in less than 2 ns, whereas the methyl radical and N_2 are significantly delayed in appearance and seem to be formed from a precursor having a lifetime of 10-14 ns. Our search for the C-H stretching spectrum of this methylidiazanyl precursor, $CH_3N=N^*$, proved unsuccessful, perhaps because of overlap with a precursor transition, an unfavorable rotational contour, or too low a Raman cross section. Nevertheless, our kinetic data provide direct evidence of stepwise dissociation

(14) Collier, S. S.; Slater, D. H.; Calvert, J. G. *Photochem. Photobiol.* **1968**, *7*, 737.

(15) Fogel, L. D.; Steel, C. *J. Am. Chem. Soc.* **1976**, *98*, 4859.

(16) Robinson, P. J.; Holbrook, K. A. *Unimolecular Reactions*; Wiley-Interscience: New York, 1972.

(17) Maier, G.; Reisenauer, H. P.; Rohde, B.; Dehnicke, K. *Chem. Ber.* **1983**, *116*, 732.

(18) (a) Mal'tsev, A. K.; Korolov, V. A.; Nefedov, O. M. *Izv. Akad. Nauk SSR, Ser. Khim.* **1982**, *10*, 2415. (b) Mal'tsev, A. K.; Korolov, V. A.; Nefedov, O. M. *Izv. Akad. Nauk SSR, Ser. Khim.* **1983**, *3*, 555.

in this unsymmetrical azoalkane.

The dimethylallyl radical appears first, as one would predict on the basis that the weaker C-N bond to the dimethylallyl group (27 kcal/mol) should rupture before the stronger C-N bond to methyl (52 kcal/mol).¹ The resulting methyldiazenyl radical persists for 10 to 14 ns under the collisional conditions used here before fragmenting into N₂ plus CH₃^{*}. This lifetime is remarkably consistent with the 11-ns value deduced for methyldiazenyl in hydrocarbon solution by Engel and Gerth³ on the basis of thermal activation parameters. Quantum chemical calculations predict that dissociation of methyldiazenyl is an exothermic but activated process with estimated barrier heights of 6.3-17.4 kcal/mol.^{5a,19} Because of this barrier, we expect that the persistence of the methyldiazenyl radical will depend strongly on its internal energy content. In the gas phase, where collisional relaxation of vibrational energy is far slower than in solution, the methyldiazenyl at early times retains the nascent excitation level with which it is formed as the first C-N bond breaks. For MAMB, the large dimethylallyl fragment has 36 vibrational modes and is able to carry away a significant fraction of the excess energy available from the 80.6-kcal/mol excitation photon. This would leave the methyldiazenyl fragment with less vibrational energy, and thus a longer lifetime, than from a similar stepwise photodissociation of azomethane. We suspect that our failure to resolve a stepwise mechanism in previous azomethane vapor studies⁸ may therefore reflect a shorter lifetime for methyldiazenyl rather than a qualitatively different dissociation mechanism. Finally, we note that since photodissociation in azoalkanes is believed to proceed from high levels of the electronic ground state populated by in-

ternal conversion,^{14,15} the stepwise process observed in MAMB should also occur in thermolysis of this compound.

Conclusions

By using time-resolved detection of primary photoproducts, we have kinetically resolved the stepwise breakage of C-N bonds in the ultraviolet-induced dissociation of an unsymmetrical azoalkane. Although the intermediate methyldiazenyl radical was not directly observed, its lifetime was inferred to be 12 ± 2 ns under our gas-phase experimental conditions. We believe that the sequential mechanism applies to thermal as well as photoinduced dissociation of this compound, since both are thought to proceed on the S₀ electronic surface. In addition, it seems quite likely that the studied compound qualitatively represents the entire class of unsymmetrical azoalkanes and that these may now confidently be viewed as dissociating sequentially rather than simultaneously.

These results do not bear directly on the homolysis mechanism of symmetric azoalkanes, such as azomethane. However, if we are able to characterize the nascent rotational and vibrational distributions of the N₂ and CH₃^{*} fragments formed from MAMB through dissociation of the methyldiazenyl radical, then these distributions may be compared to those from azomethane and the outcome used to establish or exclude a common intermediate for the two cases. These and related studies are planned for the future.

Acknowledgment. We are grateful to the National Science Foundation and the Robert A. Welch Foundation for research support. Acknowledgment is also made to the donors of the Petroleum Research Fund, administered by the American Chemical Society, for partial support of this work. R.B.W. thanks the Alfred P. Sloan Foundation for a Research Fellowship; K.A.B. thanks the A.R.C.S. Foundation for a graduate scholarship.

Registry No. MAMB, 105018-56-2; AMB, 71647-31-9.

(19) (a) Holmes, T. A.; Hutchinson, J. S., Rice University, personal communication. (b) Yamashita, K.; Kamino, M.; Yamabe, T.; Fukui, K. *Chem. Phys. Lett.* **1981**, *83*, 78.

Pyrophosphate Formation from Acetyl Phosphate and Orthophosphate Anions in Concentrated Aqueous Salt Solutions Does Not Provide Evidence for a Metaphosphate Intermediate¹

Daniel Herschlag and William P. Jencks*

Contribution No. 1603 from the Graduate Department of Biochemistry, Brandeis University, Waltham, Massachusetts 02254. Received June 3, 1986

Abstract: The formation of pyrophosphate (PPi) from the anions of acetyl phosphate (AcP) and orthophosphate (Pi) in concentrated aqueous sodium perchlorate is approximately first order in each reactant. The pH dependence of the reaction in the presence of 0.25 M Pi monoanion and 6.4 M sodium perchlorate at 54 °C shows different yields of PPi from AcP monoanion and dianion. This result is inconsistent with trapping of a free metaphosphate intermediate by Pi monoanion and water. The results are consistent with a concerted mechanism for PPi formation and yields of PPi from the different ionic species of 11.7% for AcP²⁻ and Pi²⁻, 7.8% for AcP²⁻ and Pi⁻, and 4.2% for AcP⁻ and Pi⁻. Measurement of rate constants and partitioning with AcP²⁻, 0.25 M Pi²⁻, and 6.4 M sodium perchlorate, in the presence and absence of pyridine, show that the phosphorylated pyridine monoanion yields 40% PPi, whereas AcP²⁻ yields 10% PPi under the same conditions. The formation of PPi from AcP and Pi dianions is at least fourth order in sodium ion in concentrated sodium perchlorate solutions. The corresponding reaction of the monoanions is second order in sodium ion. The order of effectiveness of salts for facilitation of the formation of PPi from the dianions of AcP and Pi is NaClO₄ > NaCl, KCl, CsCl, and NaCl > CsCl. However, increasing the concentration of sodium perchlorate from 0.1 to 6.6 M changes the rate constant for hydrolysis of AcP mono- and dianion by <30% at 39 and 54 °C. Values of $\Delta H^\ddagger = 29$ kcal mol⁻¹ and $\Delta S^\ddagger = +12$ eu for PPi formation from the dianions of AcP and Pi and $\Delta H^\ddagger = 19$ kcal mol⁻¹ and $\Delta S^\ddagger = -20$ eu for PPi formation from the monoanions were obtained from the yields of PPi and the rates of hydrolysis at 39 and 54 °C. The high concentrations of sodium ion decrease electrostatic repulsion between the anions of AcP and Pi and may catalyze the formation of PPi by bridging the anions of AcP and Pi. These results provide no evidence for the existence of a metaphosphate intermediate in reactions in aqueous solution.

The reactions of phosphate monoesters and related compounds with solvent and other nucleophilic reagents involve nearly com-

plete bond breaking with the leaving group and little bond formation to the nucleophile. For example, the rapid hydrolysis of